

Three-periodic nets and tilings: edge-transitive binodal structures

Olaf Delgado-Friedrichs,^a Michael O’Keeffe^{a*} and Omar M. Yaghi^b

^aDepartment of Chemistry and Biochemistry, Arizona State University, Tempe, AZ 85287, USA, and

^bDepartment of Chemistry and Biochemistry, University of California, Los Angeles, CA 90095, USA.

Correspondence e-mail: mokeeffe@asu.edu

28 three-periodic nets with two kinds of vertex and one kind of edge are identified. Some of their crystallographic properties and their natural tilings are described. Restrictions on site symmetry and coordination number of such nets are discussed and examples of their occurrence in crystal structures are given.

1. Introduction

In the design of crystals in which symmetrical building units are linked together in periodic arrays (*reticular chemistry*, Yaghi *et al.*, 2003), it is particularly valuable to have an inventory of structures of high symmetry as these are most likely to be produced in practice unless other low-symmetry structures are specifically targeted (Ockwig *et al.*, 2005). Structures in which all the links between modules are the same are particularly important, and these will be based on nets with one kind of edge (edge-transitive). In two earlier papers in this series (Delgado Friedrichs, O’Keeffe & Yaghi, 2003*a,b*), we identified and described 20 three-periodic nets with one kind of vertex and one kind of edge (*i.e.* vertex- and edge-transitive). We restricted ourselves to nets that had full symmetry embeddings in which the distances between unconnected vertices were not less than edge lengths, as without that restriction there are infinite families of edge- and vertex-transitive three-periodic nets with high coordination number (Delgado-Friedrichs *et al.*, 2005). 13 of those 20 nets can be colored so that black vertices are linked only to white vertices and *vice versa* with just one kind of link (Delgado Friedrichs, O’Keeffe & Yaghi, 2003*b*). Here we describe some additional nets with one kind of link, but with vertices of two different kinds (different coordination figures). We restrict ourselves to nets that have full symmetry embeddings in which the distances between unconnected unlike vertices are not less than edge lengths but, even with that restriction, we do not

claim completeness as the nets are found empirically. We do believe, however, that most of the more symmetrical such nets have been included.

We refer to the earlier papers for definitions; here we just note that we describe a net in terms of its *natural tiling*, which is one which preserves the full symmetry of the net and in which the tiles are as small as possible provided the faces are all strong rings.¹ Strong rings are those which are not the sum of smaller rings.

2. Symmetry and stoichiometry

We consider a structure with vertices *A* and *B* with coordination numbers *a* and *b*; the stoichiometry is *A_bB_a*. The order of the point symmetry at a site in a crystal is equal to the multiplicity of the general position of the space group divided by the multiplicity of that site. It follows at once that, in a particular embedding, the order of the point symmetry at *B* is *a/b* times that at *A*. For a given coordination figure (tetrahedron say), there is a maximum point symmetry with order *o* (*o* = 24 for a tetrahedron) and *n* vertices (*n* = 4 for a tetrahedron). If a structure *A_bB_a* is to be assembled with the maximum symmetry at both vertices, a necessary condition is that *o_A/n_A = o_B/n_B*.

In Table 1, we list *o/n* for a number of symmetrical shapes that can occur in structures of cubic or hexagonal symmetry. Note that the symmetry of a regular triangle, considered as a three-dimensional object, is $\bar{6}m2$ (order 12) – not possible in a cubic structure; in a cubic structure, the maximum symmetry is a subgroup of order 6 (*3m* or 32). Likewise, for an icosahedron, the maximum symmetry in a cubic crystal is $m\bar{3}$ (order 24). The possible combinations with maximal symmetry can be seen from Table 1 to be: cube/tetrahedron (realized in **flu**),

¹ This definition leads to a unique natural tiling in the simple high-symmetry nets considered here and earlier. For some lower-symmetry structures, the definition of natural tiling needs to be extended to avoid ambiguities. We will address this topic in a subsequent publication. We note that for one net, **thp**, we (Delgado Friedrichs, O’Keeffe & Yaghi, 2003*b*) missed a ring in the structure and the natural tiling is $2[3^2 4^2] + 3[4^2]$ and the dual $[6^6]$. We thank V. Blatov and D. M. Proserpio for bringing this to our attention.

Table 1

Maximum order (*o*) of symmetry divided by number of vertices (*n*) for some geometrical figures compatible with cubic or hexagonal symmetry.

Cubic symmetry	<i>o/n</i>	Hexagonal symmetry	<i>o/n</i>
Cuboctahedron	4	Hexagonal prism	2
Icosahedron	(10) 2	Trigonal prism	2
Truncated tetrahedron	2	Hexagon	4
Cube	6	Triangle	4
Octahedron	8		
Tetrahedron	6		
Square	4		
Triangle	(4) 2		

Table 2

Edge transitive nets with two vertices.

ps refers to point symmetry of order o' . sg refers to space group and trans to transitivity of the tiling.

Z	Vertex figure	Symbol	ps	o'	sg	x, y, z	Tiles	trans
3,4	Triangle	pto	$\bar{3}2$	6	$Pm\bar{3}n$	1/4, 1/4, 1/4	$3[8^4]+[8^6]$	2122
	Square		$\bar{4}m2$	8		1/4, 0, 1/2		
3,4	Triangle	tbo	$\bar{3}m$	6	$Fm\bar{3}m$	0.3333, x, x	$2[6^4]+[8^6]+[6^8.8^6]$	2123
	Rectangle		mmm	8		1/4, 0, 1/4		
3,4	Triangle	bor	$\bar{3}m$	6	$P\bar{4}3m$	0.1667, x, x	$[6^4]+[6^4.8^6]$	2122
	Tetrahedron		$\bar{4}m2$	8		1/2, 0, 0		
3,4	Triangle	ctn	$\bar{3}$	3	$I\bar{4}3d$	0.2802, x, x	$2[8^3]+3[8^3]$	2122
	Tetrahedron		$\bar{4}$	4		3/8, 0, 1/4		
3,6	Triangle	pyr	$\bar{3}$	3	$Pa\bar{3}$	0.3333, x, x	$[6^6]+2[6^3]$	2112
	Octahedron		$\bar{3}$	6		0, 0, 0		
3,6	Triangle	spn	$\bar{3}m$	6	$Fd\bar{3}m$	0.1667, x, x	$[4^6]+[4^6.12^4]$	2122
	Octahedron		$\bar{3}m$	12		0, 0, 0		
3,8	Triangle	the	$\bar{3}m$	6	$Pm\bar{3}m$	0.1667, x, x	$[4^{12}]+3[4^4.8^2]+[8^6]$	2123
	Tetragonal prism		$4/mmm$	16		1/2, 0, 0		
3,12	Triangle	tft	$\bar{3}m$	6	$F\bar{4}3m$	0.3333, x, x	$[4^6]+[6^4]+[4^6.6^4]$	2123
	Truncated tetrahedron		$\bar{4}3m$	24		0, 0, 0		
4,4	Rectangle	pts	mmm	8	$P4_2/mmc$	0, 1/2, 0	$[8^4]+[4^2.8^2]$	2132
	Tetrahedron		$\bar{4}m2$	8	$c/a = \sqrt{2}$	0, 0, 1/4		
4,4	Rectangle	pth	222	4	$P6_222$	1/2, 0, 0	$[4.8^2]+[8^3]$	2132
	Tetrahedron		222	4	$c/a = 3/\sqrt{2}$	0, 0, 1/2		
4,6	Square	soc	$4mm$	8	$Im\bar{3}m$	0.2500, 0, 0	$[4^{12}]+3[4^4.8^4]$	2122
	Octahedron		$\bar{3}m$	12		1/4, 1/4, 1/4		
4,6	Square	she	$\bar{4}m2$	8	$Im\bar{3}m$	1/2, 0, 1/4	$3[4^4.8^2]+[4^{12}.8^6]$	2122
	Hexagon		$\bar{3}m$	12		1/4, 1/4, 1/4		
4,6	Rectangle	stp	mmm	8	$P6/mmm$	1/2, 0, 1/2	$2[4^3]+[4^6.12^2]+[4^6.12^2]$	2133
	Trigonal prism		$\bar{6}m2$	12	$c/a = 1/\sqrt{6}$	1/3, 2/3, 0		
4,8	Rectangle	scu	mmm	8	$P4/mmm$	1/2, 0, 1/2	$[4^4]+[4^4.8^2]+[4^4.8^2]$	2133
	Tetragonal prism		$4/mmm$	16	$c/a = 1/\sqrt{2}$	0, 0, 0		
4,12	Rectangle	shp	mmm	8	$P6/mmm$	1/2, 0, 1/2	$[4^6]+2[4^3.6^2]+2[4^3.6^2]$	2133
	Hexagonal prism		$6/mmm$	24	$c/a = 1/\sqrt{2}$	0, 0, 0		
4,12	Square	ftw	$4/mmm$	16	$Pm\bar{3}m$	1/2, 0, 1/2	$3[4^4]+[4^{12}]$	2112
	Cuboctahedron		$m\bar{3}m$	48		0, 0, 0		
4,6	Tetrahedron	toc	$\bar{4}m2$	8	$Pn\bar{3}m$	1/4, 1/4, 3/4	$2[4^6.6^2]+[6^4]$	2122
	Octahedron		$\bar{3}m$	12		0, 0, 0		
4,6	Tetrahedron	gar	$\bar{4}$	4	$Ia\bar{3}d$	3/8, 0, 1/4	$3[4^2.8^2]+2[4^3.8^3]$	2122
	Octahedron		$\bar{3}$	6		0, 0, 0		
4,6	Tetrahedron	ibd	$\bar{4}$	4	$Ia\bar{3}d$	3/8, 0, 1/4	$3[4.6^2]+[6^6]$	2122
	Octahedron		$\bar{3}2$	6		1/8, 1/8, 1/8		
4,6	Tetrahedron	iac	222	4	$Ia\bar{3}d$	1/8, 0, 1/4	$6[4.6^2]+2[4^3]+3[6^4]$	2123
	Octahedron		$\bar{3}$	6		0, 0, 0		
4,6	Tetrahedron	ifi	222	4	$I4_132$	5/8, 0, 1/4		
	Octahedron		$\bar{3}2$	6		1/8, 1/8, 1/8		
4,8	Tetrahedron	flu	$\bar{4}3m$	24	$Fm\bar{3}m$	1/4, 1/4, 1/4	$[4^{12}]$	2111
	Cube		$m\bar{3}m$	48		0, 0, 0		
4,12	Tetrahedron	ith	$\bar{4}m2$	8	$Pm\bar{3}n$	1/2, 0, 1/4	$4[4^3]+3[4^6]$	2122
	Icosahedron		$m\bar{3}$	24		0, 0, 0		
4,24	Tetrahedron	twf	$\bar{4}m2$	8	$Im\bar{3}m$	1/2, 0, 1/4	$12[4^3]+3[4^4]+4[4^6]$	2123
	Truncated octahedron		$m\bar{3}m$	48		0, 0, 0		
6,6	Octahedron	nia	$\bar{3}m$	12	$P6_3/mmc$	0, 0, 0	$[4^3]+[4^9]$	2122
	Trigonal prism		$\bar{6}m2$	12	$c/a = \sqrt{(8/3)}$	1/3, 2/3, 1/4		
6,8	Octahedron	ocu	$\bar{3}m$	12	$Im\bar{3}m$	1/4, 1/4, 1/4	$12[4^3]+6[4^4]+[4^{12}]$	2123
	Cube		$4/mmm$	16		1/2, 0, 0		
6,12	Trigonal prism	alb	$\bar{6}m2$	12	$P6/mmm$	1/3, 2/3, 1/2	$2[4^3]+3[4^4]+3[4^4]+[4^6]$	2134
	Hexagonal prism		$6/mmm$	24	$c/a = 2/\sqrt{6}$	0, 0, 0		
6,12	Hexagon	mgc	$\bar{3}m$	12	$Fd\bar{3}m$	1/2, 1/2, 1/2	$6[4^3]+[4^6]+2[4^6]$	2123
	Truncated tetrahedron		$\bar{4}3m$	24		1/8, 1/8, 1/8		

cuboctahedron/square (**ftw**), hexagonal prism/trigonal prism (**alb**) and hexagon/triangle (**kgd**, a layer structure).

Other combinations are only possible with lowered symmetry; for example, to have a (4,6)-coordinated net based on tetrahedral and octahedral coordination, the order of the symmetry at the 6-coordinated octahedral site can be at most $2 \times 6 = 12$, and that at the tetrahedral site $2 \times 4 = 8$. This is

realized only in the net **toc**. Nature responds to the problem by having a variety of structures for compounds A_2B_3 with octahedral and tetrahedral coordination. In addition to those described here, the net (**cor**) of the corundum (Al_2O_3) structure is commonly found (O'Keeffe *et al.*, 2000). Similar remarks apply to structures AB_2 with A in octahedral coordination where the net (**rfl**) of rutile (TiO_2) is frequently found

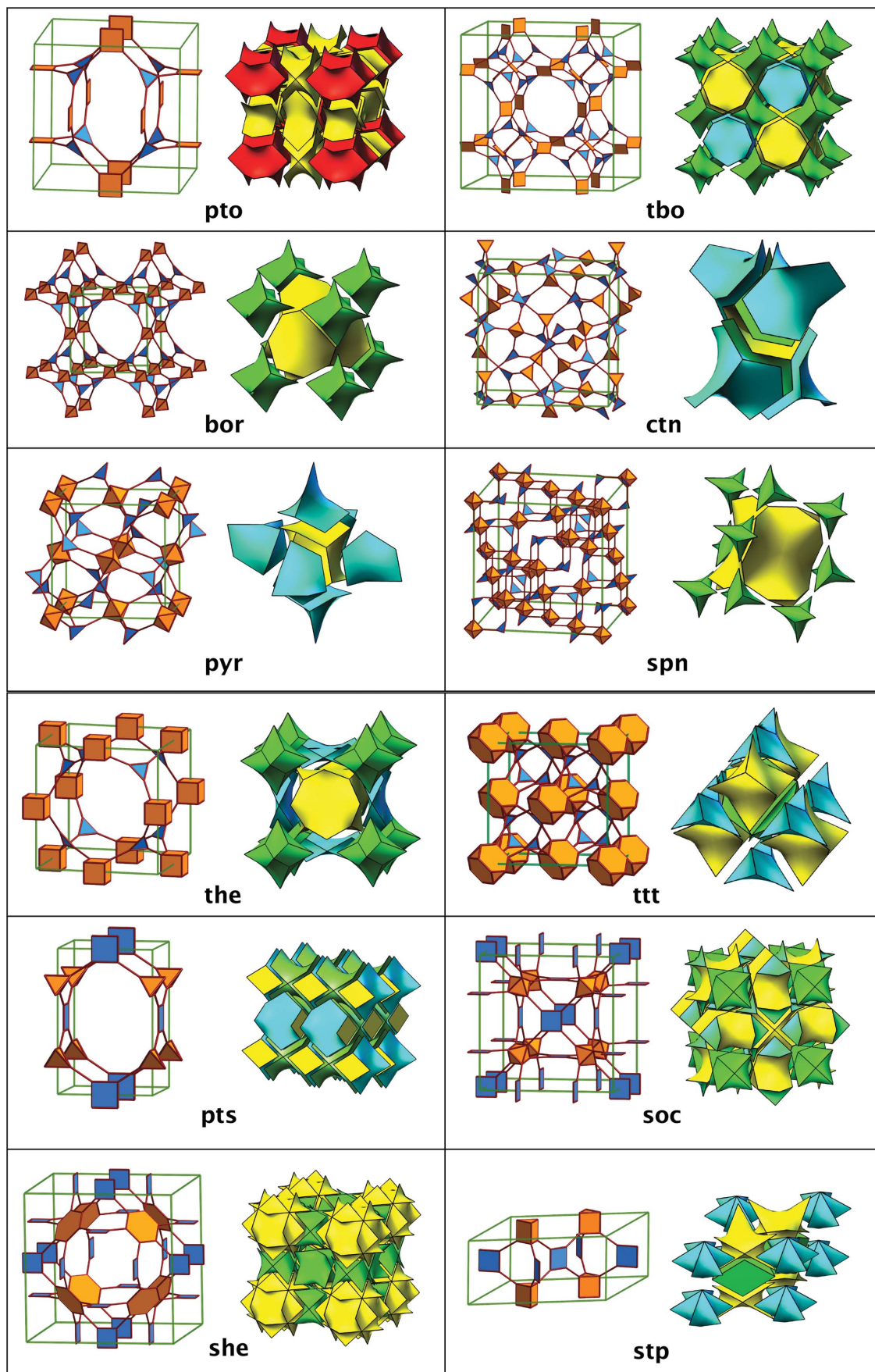


Figure 1
The nets of this paper illustrated as the augmented net (left) and as a natural tiling (right). They appear in the same order as in Table 2.

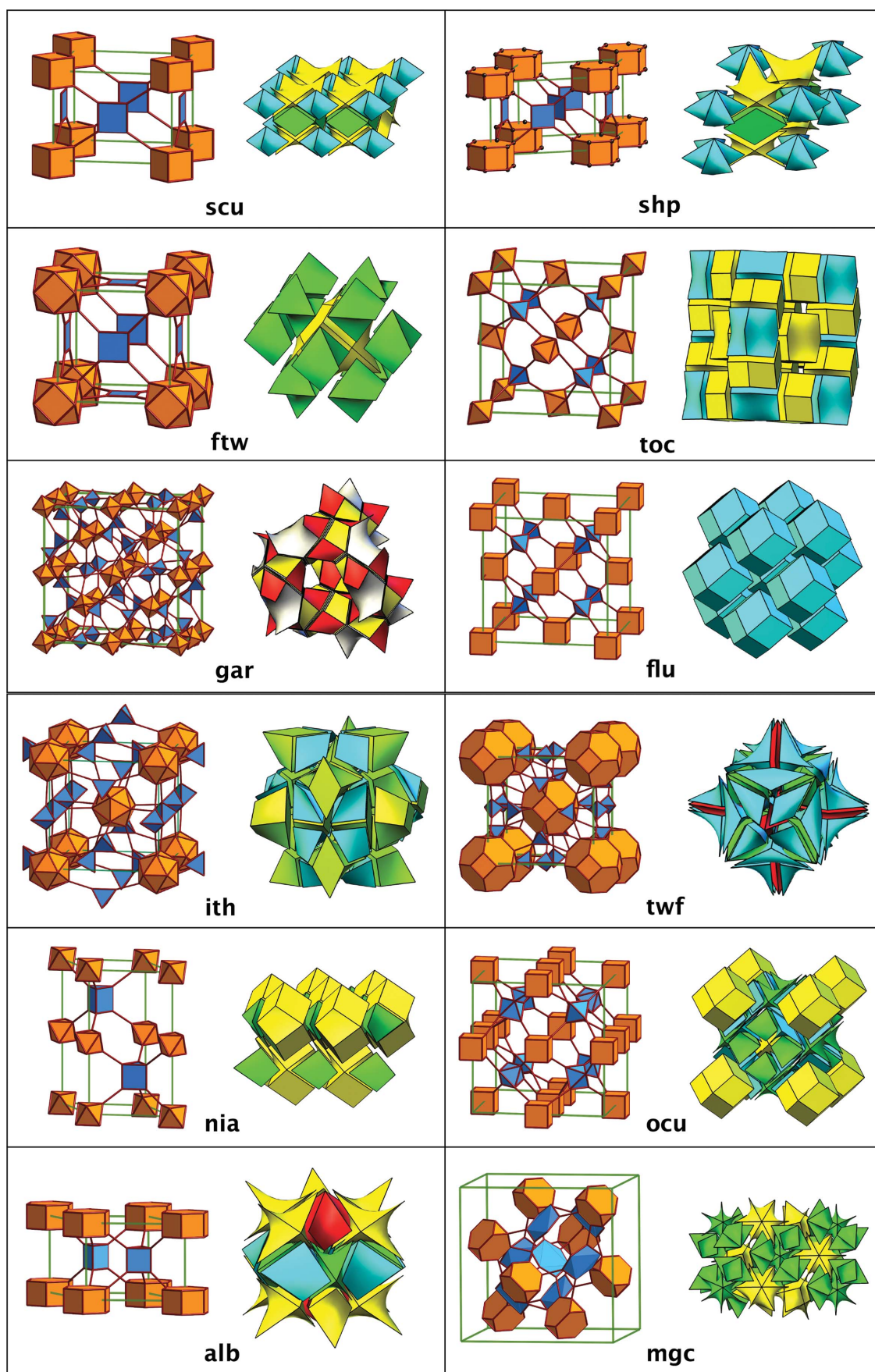


Figure 1 (continued)

Table 3

The edge nets of the nets described in this paper.

The last column is the Fischer symbol (see text) of the sphere packing with the same net. Nets are listed in the same order as in Table 2.

Number	Symbol	Edge net	Fischer
21	pto	hbo	4/3/c5
22	tbo	hal	4/3/c8
23	bor	bor-e	5/3/c7
24	ctn	ctn-e	5/3/c35
25	pyr	pyr-e	5/3/c19
26	spn	dia-j	6/3/c14
27	the	pcu-i	5/3/c8
28	tft	ubt	5/3/c4
29	pts	pts-e	5/3/r2
30	pth	wjk	5/3/h2
31	soc	bcu-k	6/3/c15
32	she	rho	4/4/c4
33	stp	ttw	5/3/h5
34	scu	fee	5/4/t4
35	shp	bnn	5/4/h5
36	ftw	reo-e	6/3/c3
37	toc	toc-e	–
38	gar	gar-e	–
39	ibd	–	–
40	iac	iac-e	–
41	ifi	–	–
42	flu	flu-e	6/3/c4
43	ith	ith-e	–
44	twf	twf-e	–
45	nia	nia-e	7/3/h20
46	ocu	ocu-e	–
47	alb	tfs	6/3/h20
48	mge	fnf	5/3/c11

(O’Keeffe *et al.*, 2000; Delgado-Friedrichs, O’Keeffe & Yaghi, 2003c). Both of these last two structures have two kinds of edge.

3. Descriptions of the structures

Crystallographic and other data for the structures are listed in Table 2. In accord with our earlier practice (Delgado Friedrichs, O’Keeffe & Yaghi, 2003a,b), each structure is assigned a symbol consisting of lower-case letters.² Tiles of tilings are described by face symbols [$M^m.N^n \dots$], which indicate that the tile has m faces that are M -gons, n that are N -gons *etc.* The *transitivity pqrs* indicates that the tiling has p kinds of vertex, q kinds of edge, r kinds of face and s kinds of tile. Clearly all the structures in the table have transitivity 21rs. Most of them are illustrated in two ways in Fig. 1: as natural tilings and as the augmented nets. In the latter, each vertex is replaced by its vertex figure; so, for example, the (4,8)-coordinated **flu** net is shown as linked cubes and tetrahedra as might appear in a structure constructed of these building units. The symbol for the augmented net is **flu-a**. Three of the 4,6-coordinated nets (**ifi**, **ibd** and **iac**) are not illustrated as they are hard to appreciate from figures. For **ifi**, we have not found a natural tiling. Net **pth** is also not illustrated – it is a lower-symmetry hexagonal variant of **pts** (see also below).

² The symbols can be used to find these structures in a database of periodic nets at <http://okeeffe-ws1.la.asu.edu/RCSR/home.htm>.

As there is only one kind of edge, the *edge nets*, derived by placing a vertex in the middle of each edge and discarding the original vertices, are uninodal. They are listed in Table 3. Many can be realized as sphere packings; in that case, the Fischer symbol (Fischer, 2004, 2005; Sowa & Koch, 2005) is also given (notice that the first number of that symbol is the coordination number). It is interesting that the edge net of **tft** has higher symmetry ($Fm\bar{3}m$) than its parent ($F\bar{4}3m$). The nets are also given a serial number in the table. These follow on from the numbers of the vertex- and edge-transitive nets (numbers 1–20).

4. Occurrences and properties

A crystal structure based on the **pto** (Pt_3O_4) net *interwoven* (rather than interpenetrating and catenated) with another copy was described by Chen *et al.* (2001).

Occurrences in crystal structures of nets **tbo** (twisted boracite), **bor** (boracite) and **soc** (square-octahedron) are detailed in O’Keeffe *et al.* (2000).

An occurrence of the net **ctn** (a hypothetical C_3N_4 structure) and a discussion of its properties and propensity for intergrowth have been given by Dybtsev *et al.* (2004).

The net **pyr** (pyrite) has similarly been described by Chae *et al.* (2003) who also found the net intergrown.

The **spn** (spinel) net is the net of the anions and octahedral cations in spinel, *i.e.* the Al and O in $MgAl_2O_4$ and Pr and I in PrI_2 . For other examples of its occurrence, see Baburin *et al.* (2005).

The net **pts** (PtS) may be derived as the edge net of the minimal net **cds** ($CdSO_4$). The related net **pth** is similarly derived from the **qzd** net. These nets and their occurrences are described by Delgado-Friedrichs, O’Keeffe & Yaghi, (2003c).

The net **gar** (garnet) is derived from the tetrahedral and octahedral anions of garnet, *i.e.* Al and Si in $Ca_3Al_2Si_3O_{12}$ as vertices and with $-O-$ links acting as edges. An imidazolate based on this topology was recently described by Park *et al.* (2006).

The **flu** (fluorite) net is the net of the atoms in fluorite (CaF_2) and of course very familiar in crystal chemistry.

The **alb** (AlB_2) net is that net of the Al–B bonds in AlB_2 – the prototype of a very large family of intermetallic compounds.

The **mge** ($MgCu_2$) net is that of the Mg–Cu bonds in $MgCu_2$ – the prototype of the largest family of intermetallic compounds.

The nets **pyr** and **ftw** have self-dual natural tilings (notice that the transitivity 2112 is palindromic). These nets are the labyrinth nets of the minimal balance surfaces $C(S)$ and $C(P)$, respectively (Fischer & Koch, 1989); *i.e.* two interpenetrating nets of each type run along the centers of the labyrinths of each surface. **mge** has a self-dual tiling (not natural), $2[4^6]+[4^{12}]$, with the same transitivity; this is in fact the tiling shown in Fig. 1. The larger tile in this tiling is formed by gluing together a $[4^6]$ and $6[4^3]$ of the natural tiling. **mge** is the labyrinth net of the $C(D)$ minimal balance surface (Fischer & Koch, 1989). The natural tiling of **ctn** has two kinds of eight-

ring face and may be written $2[8_a^3]+3[8_a^2.8_b]$. If the 8_b face (yellow in Fig. 1) is not used, one gets a self-dual (not *natural*) tiling $4[8_a^3]+3[8_a^4]$ with the same symmetry and with transitivity 2112. The net is the labyrinth net of the *S* minimal balance surface (Fischer & Koch, 1989). The four nets of this paragraph are the only ones we know of that have self-dual tilings with the symmetry of the net and that have transitivity 2112. Self-dual natural tilings with transitivity 1111 are the tilings of the nets **srs**, **dia** and **pcu** (Delgado Friedrichs, O'Keeffe & Yaghi, 2003a), which are the labyrinth nets of the *G*, *D* and *P* minimal surfaces.

This work was supported by the US National Science Foundation (grant No. DMR 0451443) and by the donors of the American Chemical Society Petroleum Research Fund.

References

- Baburin, I. A., Blatov, V. A., Carlucci, L., Ciani, G. & Proserpio, D. M. (2005). *J. Solid State Chem.* **178**, 2452–2474.
- Chae, H. K., Kim, J., Delgado Friedrichs, O., O'Keeffe, M. & Yaghi, O. M. (2003). *Angew. Chem.* **42**, 3807–3909.
- Chen, B., Eddaoudi, M., Hyde, S. T., O'Keeffe, M. & Yaghi, O. M. (2001). *Science*, **291**, 1021–1023.
- Delgado-Friedrichs, O., Foster, M. D., O'Keeffe, M., Proserpio, D. M., Treacy, M. M. J. & Yaghi, O. M. (2005). *J. Solid State Chem.* **178**, 2533–2554.
- Delgado Friedrichs, O., O'Keeffe, M. & Yaghi, O. M. (2003a). *Acta Cryst.* **A59**, 22–27.
- Delgado Friedrichs, O., O'Keeffe, M. & Yaghi, O. M. (2003b). *Acta Cryst.* **A59**, 515–525.
- Delgado-Friedrichs, O., O'Keeffe, M. & Yaghi, O. M. (2003c). *Solid State Sci.* **5**, 73–78.
- Dybtsev, D. N., Chun, H. & Kim, K. (2004). *Chem. Commun.* pp. 1594–1595.
- Fischer, W. (2004). *Acta Cryst.* **A60**, 246–249.
- Fischer, W. (2005). *Acta Cryst.* **A61**, 435–441.
- Fischer, W. & Koch, E. (1989). *Acta Cryst.* **A45**, 726–732.
- Ockwig, N. W., Delgado-Friedrichs, O., O'Keeffe, M. & Yaghi, O. M. (2005). *Acc. Chem. Res.* **38**, 176–182.
- O'Keeffe, M., Eddaoudi, M., Li, H., Reineke, T. M. & Yaghi, O. M. (2000). *J. Solid State Chem.* **152**, 2–20.
- Park, K., Ni, Z., Côté, A. P., Choi, J.-T., Uribe-Romo, F. J., Chae, H. K., Huang, R., O'Keeffe, M. & Yaghi, O. M. (2006). *Proc. Natl Acad. Sci. USA*, **103**, 10186–10191.
- Sowa, H. & Koch, E. (2005). *Acta Cryst.* **A61**, 331–342.
- Yaghi, O. M., O'Keeffe, M., Ockwig, N. W., Chae, H. K., Eddaoudi, M. & Kim, J. (2003). *Nature (London)*, **423**, 705–714.